

ORIGINAL ARTICLE

A novel approach to PTSD modeling in rats reveals alternating patterns of limbic activity in different types of stress reaction

G Ritov^{1,2}, B Boltyansky^{1,2} and G Richter-Levin^{1,2,3}

Human reactions to trauma exposure are extremely diverse, with some individuals exhibiting only time-limited distress and others qualifying for posttraumatic stress disorder diagnosis (PTSD). Furthermore, whereas most PTSD patients mainly display fear-based symptoms, a minority of patients display a co-morbid anhedonic phenotype. We employed an individual profiling approach to model these intriguing facets of the psychiatric condition in underwater-trauma exposed rats. Based on long-term assessments of anxiety-like and anhedonic behaviors, our analysis uncovered three separate phenotypes of stress response; an anxious, fear-based (38%), a co-morbid, fear-anhedonic (15%), and an exposed-unaffected group (47%). Immunohistochemical assessments for cellular activation (c-Fos) and activation of inhibition (c-Fos+GAD67) revealed a differential involvement of limbic regions and distinct co-activity patterns for each of these phenotypes, validating the behavioral categorization. In accordance with recent neurocognitive hypotheses for posttraumatic depression, we show that enhanced pretrauma anxiety predicts the progression of posttraumatic anhedonia only in the fear-anhedonic phenotype.

Molecular Psychiatry (2016) **21**, 630–641; doi:10.1038/mp.2015.169; published online 10 November 2015

INTRODUCTION

Long-term reactions to trauma are extremely diverse. Some people exposed to an extreme traumatic event exhibit only time-limited distress and remember it without an excessive emotional response. Others, exposed to the same event, might continue to intrusively re-experience it and consequently qualify for a diagnosis of posttraumatic stress disorder (PTSD). This pathological reaction to trauma is generally accompanied by a range of distress symptoms, including hyperarousal, negative mood alterations and avoidance of trauma reminders. The prevalence of different long-term responses to trauma and their synergic features are quite variable among different PTSD patients. Although many sufferers exhibit mostly fear-based symptoms, some may demonstrate a more anhedonic or dysphoric phenotype.¹ However, unlike other anxiety and mood-based disorders accompanied by similar characteristics, the core criteria for the diagnosis of PTSD necessitate the occurrence of an external traumatic event as a reference point for the onset of the symptoms. Seminal progression of PTSD was therefore suggested to evolve from the associations formed during the traumatic situation itself and their subsequent consolidation, accordingly ascribing it as a memory-related disorder.^{2,3} Intrusive and aversive recollections, prominent symptom of PTSD, allegedly develop from over-consolidation of emotions associated with the trauma and their subsequent resistance to extinction over time.^{4,5} The recalling of trauma-related emotions through intrusive thoughts and flashbacks is very different from the recall of other emotional memories. Unexpectedly triggered by internal or external cues, such flashbacks are often experienced by PTSD patients as mere fragments of the emotions that accompanied the trauma.^{6,7} These unique characteristics may imply that involuntary recollections of trauma-related emotions in PTSD is further induced through fundamental dysfunctions in processes of memory

retrieval,⁸ which seminally shape the progression of individual trauma response, and subsequent sequela subtypes.⁹

At the neurobiological level, PTSD is often conceptualized in terms of excessive conditioned fear, mediated by the activation and connectivity of fear processing limbic regions, such as the amygdala, hippocampus and the medial prefrontal cortex (mPFC). Hyper-responsivity of the amygdala and mPFC is suggested to mediate fear generation^{10,11} and consequently account for the hyperarousal symptoms in PTSD.¹² Poor connectivity between the hippocampus and mPFC can lead to impaired fear inhibition^{11,13} and is suggested to account for symptoms of re-experiencing and avoidance.¹² Additionally, different extremes of inter-regional regulation within this circuitry are suggested to account for the wide-scale diversity in trauma responses, or subtypes, observed in PTSD.¹⁴ According to this, failure of amygdala inhibition due to low mPFC activation is associated with under-modulation of emotion and a more anxious, fear-based phenotype. In contrast, increased activation of the mPFC and hyper-inhibition of the amygdala is associated with over-modulation of emotion and the more anhedonic or dysphoric-based phenotype.⁹ However, these interpretations mainly relay on low-resolution data of imaging studies in humans, which are unable to detect the microanatomy of the mPFC–amygdala–hippocampus circuitry, as well as distinguish between excitatory projections and activation of inhibitory interneurons.¹⁵ Further understanding of the interrelations within this circuitry and their possible function in different types of response to trauma require the additional use of complementally research approaches.

In basic research, Pavlovian fear conditioning is commonly used in rodents to model and elucidate different aspects of PTSD. In this paradigm, animals are initially trained to associate a novel cue or context with a fear-inducing stimulus, such as foot shock. Following these pairings, exposing animals with only the cue

¹Sagol Department of Neurobiology, University of Haifa, Haifa, Israel; ²The Institute for the Study of Affective Neuroscience, University of Haifa, Haifa, Israel and ³Psychology Department, University of Haifa, Haifa, Israel. Correspondence: Professor G Richter-Levin, Sagol Department of Neurobiology, University of Haifa, Haifa 31905, Israel. E-mail: galrichterlevin@gmail.com

Received 17 June 2015; revised 1 September 2015; accepted 14 September 2015; published online 10 November 2015

while measuring stereotypic behavioral responses (such as mobility or exploration) enables the assessment of associative learning of fear and its neural implications.¹¹ However, in most animal studies, fear response to the presentation of the reminder cue is evaluated as an expression of the dichotomist effect of the exposure variable, regardless of variations in individual response.^{16,17} According to this, indications for a pathological-like response are generally inferred from significant differences in the average of the behavior assessed, when compared between exposed and non-exposed populations. As a result of such deduction process, fear condition models in rodents frequently fail to mimic the diverse facets of the human reaction to trauma.^{18,19} Thus the intriguing divergence of symptom characteristics observed in the different phenotypes of PTSD, and their potential neural correlates, are not presented in current PTSD models in rodents.

In order to address this gap, we initially exposed adult male rats to an extreme stress in the underwater trauma (UWT) model^{20–24} and used novel behavioral assessments to measure long-term alterations in their hedonic and fear responses (for details, see Supplementary Figure S1). An individual profiling approach was then implemented to analyze these assessments and screen for possible phenotypes of stress response, revealing the existence of three distinct behavioral sub-groups; an affected anxious, fear-based subtype; an affected co-morbid, fear-anhedonia subtype; and an exposed-unaffected group. We then used dual-label immunohistochemistry to specify the involvement of emotion-processing limbic areas in these different behavioral subtypes during their exposure to a contextual reminder. Expression of c-Fos, as a marker for neuronal activity, and co-labeling of the GAD67 indicator for GABAergic cells were used to evaluate the activity in the mPFC–amygdala–hippocampus circuit, as well as in areas conveying its basic fear information, as the periaqueductal gray (PAG),^{25,26} and pleasure, as the nucleus accumbens (NA).^{27,28} As interconnectivity within this circuitry is suggested to influence individual trauma responses, regional co-activation patterns in the different phenotypes were further modeled at the network level. We then evaluated prominent variations in the patterns of the affected phenotypes in light of neurocognitive hypotheses of network dysregulation as an alternator of symptom profiles in PTSD⁹ and as key contributor to the development of posttraumatic depression.²⁹

MATERIALS AND METHODS

Subjects

Forty-six adult male Sprague Dawley rats (8–9 weeks old) weighing 250–275 g (Harlan, Jerusalem, Israel) at arrival were habituated in the laboratory vivarium for 5 days. Animals were housed two per cage in a temperature-controlled (23 °C ± 1 °C) animal quarters on a 12:12-h light–dark cycle (lights on at 0700–1900 hours). They had *ad libitum* access to standard rodent chow pellets and water.

Behavioral protocols

Water-associated zero maze (WAZM). The WAZM is a transformation of the elevated zero maze to an integrated wet and dry context (see Supplementary Figure S1a; for further details of this apparatus, see Ritov and Richter-Levin³⁰). This apparatus enables the formation of an association of the maze with an UWT, and by that, the assessment of complex behaviors during re-exposure to the context which immediately precedes a traumatic experience. For the tests, rats were first habituated to the room for 2 min and then were placed into one of the open arms facing a closed part of the apparatus. Rats were allowed to explore the arena for a 5-min session. During this time, rats' behavior was tracked, recorded and analyzed by the Etho-Vision system (Noldus Information Technology, Wageningen, The Netherlands). Behavioral measures included the time spent in the open arms, distance traveled in the open arms, distance traveled in the closed arms and total freezing.

UWT stress

Animals were randomly assigned to either control or UWT conditions. The UWT stress was carried out immediately after the fourth habituation. UWT rats were lifted from the dry arms, placed in the aquatic center of the WAZM (containing water at 22 °C ± 2 °C, 50 cm deep) and submerged under water for 45 s, using a special metal net (20 × 10 × 15 cm³). After the procedure, the animals were dried briefly and returned to their housing cages. This procedure is known to acutely and enduringly increase anxiety-like behavior^{20,21,23,24} without any tissue damage.²² The procedure did not cause any loss of life or changes in body weight compared with control.

Continuous saccharine preference (CSP) test

The CSP test enables a fine measurement of consumption behavior over a long period of time without the need for water deprivation, single housing or interruption of transferring to a test cage. Beginning with the ninth day of the experiment, all rats were placed in a home cage suited for the CSP. In this apparatus, animals are held two in a cage, with a perforated partition separating between them (see Supplementary Figure S1b). The perforated separation enables a level of social interaction but separates the use of two sets of two burettes (one filled with water and the other with 0.03 mg l⁻¹ saccharine), thus enabling to continuously follow the individual saccharine preference for each animal.

Experimental procedures

In this study, identical behavioral procedures were repetitively performed for six times on consecutive batches (*n* = 8 each). Illustrated in Supplementary Figure S1c, all rats were initially habituated to the context of the WAZM using four consecutive daily exposures to a 5-min testing. Only at the beginning of the fourth day habituation, rats were randomly assigned to one of the two experimental conditions. In the UWT condition (UWT; *n* = 34), rats were exposed to the testing and immediately after the UWT stress of 45-s restrain under water in the WAZM center. In the control condition ('control'; *n* = 12), rats were exposed to testing and immediately returned to their housing cages. During the next 27 days, rat's saccharin preference was measured every third day. On the thirty-first day, all rats were re-exposed to the WAZM test as a contextual reminder by a blind experimenter. Habituation procedures and replenishment of saccharin were performed between 1000 and 1700 hours. As long-term responses to stress were shown to be significantly affected by the time at which the exposure occurred,³¹ the UWT exposures were consistently conducted between 1100 and 1400 hours throughout the experiments. All experimental procedures performed adhered to the NIH Guide for the care and use of laboratory animals and were approved by the University of Haifa ethical committee.

Behavioral profiling

This analysis was based on the within-group variability of animals behavior in order to establish distinct profiles of altered behaviors. Classification criteria were defined according to the control group distribution. The different criteria relied on the upper or lower 20th percentiles of control's anxious-like (fear responses in the WAZM) and anhedonic (averaged assement in the CSP) behaviors.

Individual profiling according to anxious-like behaviors. Group means indicated that on the thirty-first day UWT rats spent significantly less time and traveled less distance in the open arms of the maze and spent significantly more time freezing but did not differ significantly from control rats in the distance moved in the closed arms (Figures 1b–e). A 20th or 80th percentile criteria was then set in accordance with control's distribution for each behavior (dashed gray line in Figures 1b–e). Every individual rat that demonstrated a behavior that crosses this criteria got a score for being 'affected' on that single behavior (lower than 20th percentile for time spent in the open arms and distance traveled in the open and closed arms; higher than 80th percentile for time freezing). When a rat got three 'affected' scores out of the four assessments for anxious-like behavior, it was classified as an affected anxious rat.

Individual profiling according to anhedonic behavior. Group means indicated that control and UWT rats have a similar average consumption of saccharin (Figure 1f). A 20th percentile criterion was then set in accordance with control's distribution (dashed gray line in Figure 1f). Every individual UWT rat that demonstrated a behavior that does not cross this

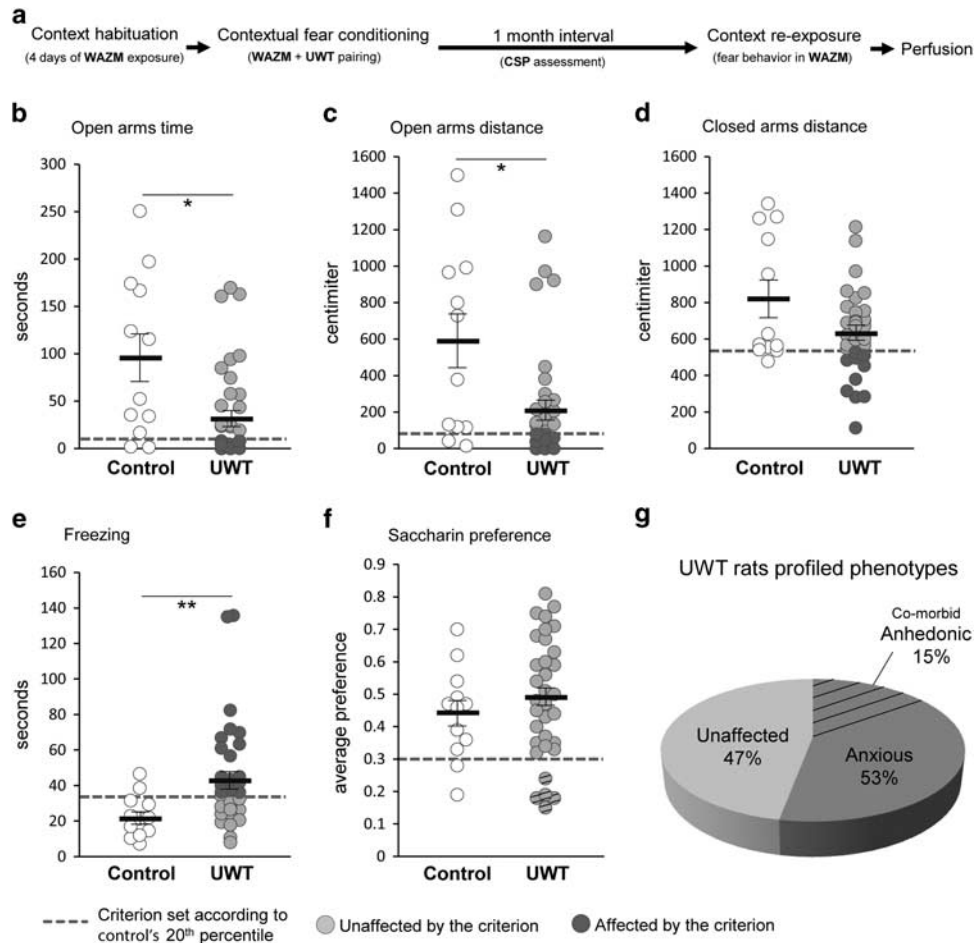


Figure 1. One month after conditioning, averaged reactions to contextual reminders of underwater trauma (UWT) are increased, yet a profiling approach reveals a fundamental diversity in the individual responses of exposed rats. **(a)** Timeline of the experiment (see also Supplementary Figure S1c). Re-exposure to the water-associated zero maze (WAZM) test as a contextual reminder of UWT extensively affects anxious-like behavior. UWT rats ($n = 34$) spent significantly less time **(b)** and traveled less distance **(c)** in the open arms of the maze, yet did not differ significantly from control rats ($n = 12$) in the distance traveled in the closed arms **(d)**. **(e)** UWT rats spent significantly more time freezing during the WAZM re-exposure. **(f)** UWT rats did not differ significantly from control rats in the average preference of saccharin. Black bars represent the groups mean \pm s.e.m.; * $P < 0.05$; ** $P < 0.01$. **(g)** Individual profiling was conducted using the control's group distribution. The profiling criteria based on the 20th percentile (dashed gray line) of both anxious-like behaviors (a minimum of three affected criteria in panels **b**, **c**, **d** or **e**) and anhedonia assessment **(f)**. The combined profiling classification identified two different categories of affected style among UWT rats, affected anxious ($n = 11$), affected anhedonic ($n = 5$) and an additional exposed-unaffected group ($n = 16$). CSP, continuance saccharin preference assessment.

criterion got a score for being anhedonic and was classified as an affected anhedonic rat.

Final classification. Anxiety-based profiling and anhedonic-based profiling were combined together among all rats. As shown in Figure 1g, this revealed three different categories of reaction style among UWT rats: an affected, clear anxious phenotype ($n = 13$), a co-morbid, anxious and anhedonic, affected phenotype ($n = 5$), and an additional exposed-unaffected group ($n = 16$).

Immunohistochemistry

Ninety minutes after the onset of the contextual reminder, rats were anesthetized with an overdose of sodium pentobarbital (CTS, Kiryat Malachi, Israel) and perfused intracardially with ice-cold saline followed by 4% paraformaldehyde in 0.1 M phosphate-buffered saline (PBS; pH 7.4). The brains were removed and stored in the same fixative for 24 h at 4 °C and subsequently immersed in 30% sucrose at 4 °C. Brains were then frozen in powdered dry ice and stored at -80 °C until sectioning. Coronal sections (30 μ m) containing relevant regions were cut using a cryostat (Leica Microsystems, Wetzlar, Germany) at -20 °C and collected in PBS for immunohistochemical processing.

Free-floating sections were washed (three times for 10 min each) in PBS and incubated for 15 min in Background Sniper (Biocare Medical, Concord, CA, USA). Sections were then incubated with the primary antibodies for c-Fos and GAD67 (rabbit anti c-Fos: 1:1000 dilution, Cell Signaling Technology, Danvers, MA, USA, catalog no. 22505; mouse anti GAD67: 1:400, EMD Millipore, Billerica, MA, USA, catalog no. MAB5406) in 3% bovine serum albumin in PBS with 0.3% Triton X-100 (PBST) for 1.5 h on a shaker at room temperature followed by an overnight incubation at 4 °C. On the next day, sections were washed (three times for 10 min each) in PBS and incubated on a shaker for 1 h with the secondary antibody Alexa Fluor 488 and Alexa Fluor 555 (1:1000 dilution, Invitrogen, Waltham, MA, USA) in PBST at room temperature. Finally, sections were washed in PBS, mounted on gelatin-coated slides, air-dried and coverslipped with Gel Mount (Sigma-Aldrich, Rehovot, Israel).

Fluorescent images were taken with a Zeiss AxioScope.A1 (Carl Zeiss, Jena, Germany) equipped with a digital camera AxioCam MRc (Carl Zeiss) using a $\times 10$ objective. Labeled immunoreactive cells were quantified bilaterally and averaged from three different sections containing relevant regions for each rat. Sampled areas were about 1 mm², and the number of labeled cells was manually counted in a blind manner using the ZEN lite 2012 software (Carl Zeiss).

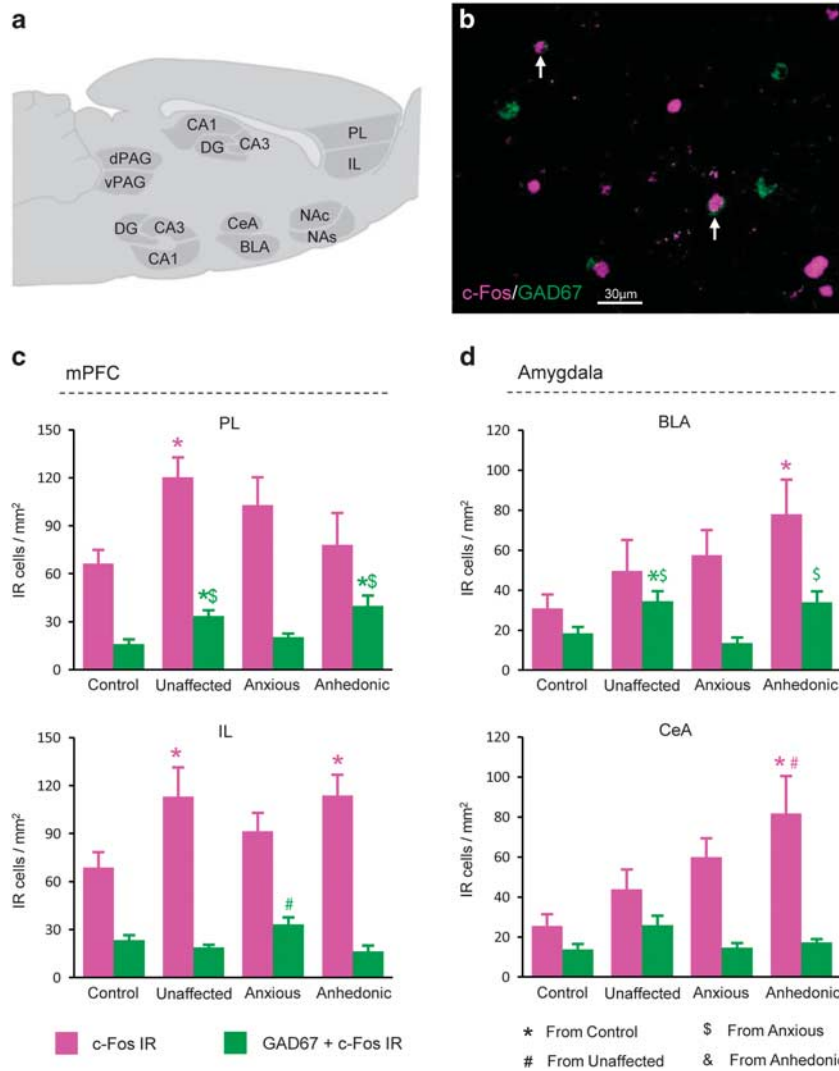


Figure 2. Differential activation of medial prefrontal cortex (mPFC) and amygdala in the different phenotypes of underwater trauma (UWT) and control rats. **(a)** Diagram of analyzed regions. Labeled cells were quantified bilaterally and averaged from $3 \times 30 \mu\text{m}$ sections per region. **(b)** An example of dual-colored immunohistochemical labeling for c-Fos expression (magenta) as a biochemical marker of cellular activation and GAD67 (green) as a biochemical marker of inhibitory GABAergic cells in the BLA. White arrows point to dual-labeled (DL) cells, co-expressing GAD67 and c-Fos, which are considered as activation of inhibition. **(c)** Differences in activation (total c-Fos-expressing cells) and activation of inhibition (DL cell count) in the sub-divisions of the mPFC between the different phenotypes of UWT and control rats. **(d)** Differences in activation and activation of inhibition in the BLA and CeA nuclei of the amygdala between the different phenotypes of UWT and control rats. Bars represent the groups mean \pm s.e.m. Significant Bonferroni *post-hoc* results with $P < 0.05$ are flagged as: *different from control; #different from unaffected; \$different from affected anxious; & different from affected anhedonic. BLA, basolateral amygdala; CeA, central amygdala; IL, infralimbic cortex; PL, perirhinal cortex.

Statistical analysis

Data were analyzed using the IBM SPSS Statistics Software (IBM, Armonk, NY, USA). Shapiro–Wilk test of normality and Levene’s test for homogeneity of variance were utilized for inclusion in parametric tests. No animals were excluded from the behavioral analysis ($n = 46$), yet a total of 4 brain samples were lost owing to bad perfusion and excluded from the immunohistochemical analysis. Two-tailed *t*-tests were used for initial comparisons between control and UWT rats. Following the individual profiling classification, one-way analysis of variance (ANOVA) with Bonferroni *post-hoc* ($P < 0.05$) was used to compare group means. Linear regression and two-tailed Pearson test were used to assess relations and were considered significant when $P < 0.05$.

Multidimensional scaling analysis (MDS). MDS refers to a family of algorithms that operate on multiple measurements basing on data similarity to create proximities. The output of MDS is a configuration of

objects embedded in a multidimensional space. It is used in many research fields to explore the inner structures within complex data such as object perception and mental representation in cognitive psychology.^{32,33} In this study, normalized excitation data (Z-scores) were analyzed using the SPSS ALSCAL MDS to create Euclidean distances from the Z-score of regional excitations and a metric space of simultaneous excitation similarities. Kruskal’s STRESS was used for a goodness-of-fit measure with a < 0.1 value threshold. R-square represents the proportion of variance accounted for by the MDS procedure.

RESULTS

UWT affects long-term reactions to contextual reminders

To evaluate the long-term effects of extreme stress exposure, we employed a contextual fear conditioning protocol using the

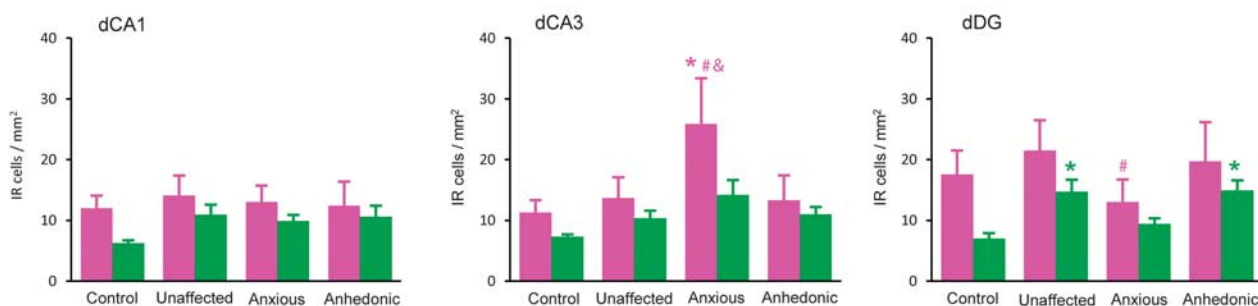
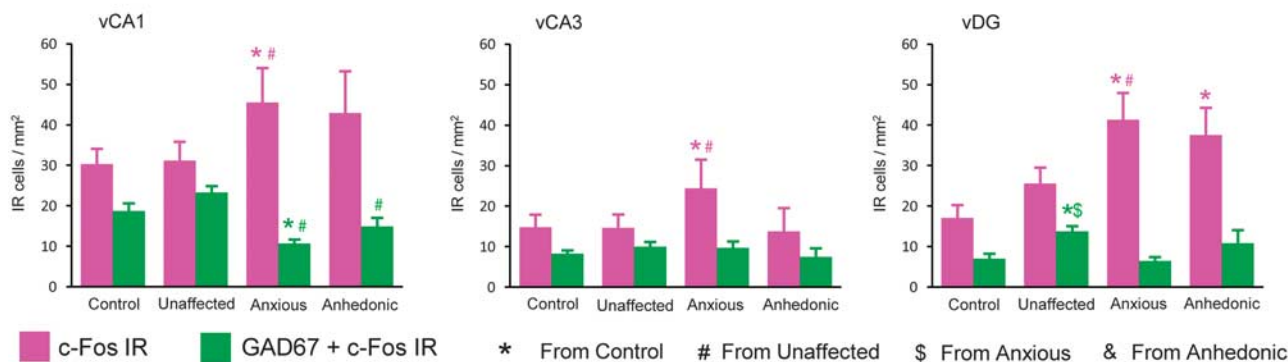
a Dorsal Hippocampus**b Ventral Hippocampus**

Figure 3. Differential activation of dorsal and ventral hippocampus in the different phenotypes of underwater trauma (UWT) and control rats. **(a)** Differences in activation (total c-Fos-expressing cells) and activation of inhibition (dual-labeled (DL) cell count) in the dorsal hippocampus layers between the different phenotypes of UWT and control rats. **(b)** Differences in activation (total c-Fos expressing cells) and activation of inhibition (DL cell count) in the ventral hippocampus layers between the different phenotypes of UWT and control rats. Bars represent the groups mean \pm s.e.m. Significant Bonferroni *post-hoc* results with $P < 0.05$ are flagged as: *different from control; #different from unaffected; \$different from affected anxious; and &different from affected anhedonic. d/vCA1, dorsal/ventral cornus ammonis 1; d/vCA3, dorsal/ventral cornus ammonis 3; d/vDG, dorsal/ventral dentate gyrus.

WAZM model.³⁰ Following 4 days of habituation to the maze, test rats (UWT) were exposed to an UWT stress in the aquatic center of the WAZM (for further details, see Supplementary Figure S1). No differences were found between the behavior of control and UWT rats before this pairing (see Supplementary Figures S2a–d). One month after the conditioning, all rats were re-exposed to the WAZM test as a contextual reminder. Analyses of rats' fear response during this contextual re-exposure revealed significant differences between the control and UWT groups in the time spent in the open arms ($t_{(44)} = 2.4$, $P < 0.05$; Figure 1b), distance traveled in the open arms ($t_{(44)} = 2.4$, $P < 0.05$; Figure 1c) and total freezing ($t_{(44)} = 3.5$, $P < 0.01$; Figure 1e). With regard to the safer areas of the maze, control and UWT rats did not differ significantly in the distance traveled in the closed arms ($t_{(44)} = 1.7$, $P > 0.11$; Figure 1d). Hedonic behavior over a long period of time was analyzed using the CSP test (see Supplementary Figure S1b). Assessment of average saccharin preference during the 4-week interval between the UWT and the context re-exposure revealed no significant between-group effects ($t_{(44)} = 0.13$, $P > 0.9$; Figure 1f).

Individual profiling classification reveals different subtypes of stress response in rats

In order to profile altered behaviors within the variability of the study population, anxious-like behavior in the WAZM and hedonic behavior in the CSP were categorized according to the control group distribution.¹⁷ Determination of the classification criteria was based on the lower 20th percentiles of control's distribution for

time spent in the open arms (< 10.88 s), distance traveled in the open arms (< 86.9 cm) and distance traveled in the closed arms (< 539 cm) during the context of re-exposure, as well as average saccharin preference in the CSP test (< 0.3 ratio). For determination of the freezing criterion, the classification was based on the upper 20th percentile of control's distribution (> 34.4 s). Rats were then individually discerned for each of the single criterion (Figures 1b–f). For anxious-like behavior classification, every rat that demonstrated a behavior profile that falls within a minimum of three out of the four criteria of fear behaviors in the WAZM was classified as an affected anxious ($n = 18$; Figure 1g). Rats were then discerned for anhedonic behavior. Every individual rat that demonstrated a behavior that does not cross the criteria for average saccharin preference in the CSP test (that is, < 0.3 ratio) got an additional score for being anhedonic (Figure 1f). The final classification combined the anxious-like and anhedonic profiling by discerning every individual rat for falling within the criteria of affected anxious alone, anhedonic alone or both. As depicted in Figure 1g, this final classification revealed two different subtypes of affected style among rats exposed to UWT: an affected fear-based anxious phenotype and an affected co-morbid anhedonic phenotype, with an additional exposed unaffected group.

Altered activation of emotion-processing regions in different subtypes of affected style

We initially assessed the activation in the sub-regions of the mPFC, NA, amygdala, hippocampus and PAG (Figure 2a) in the different

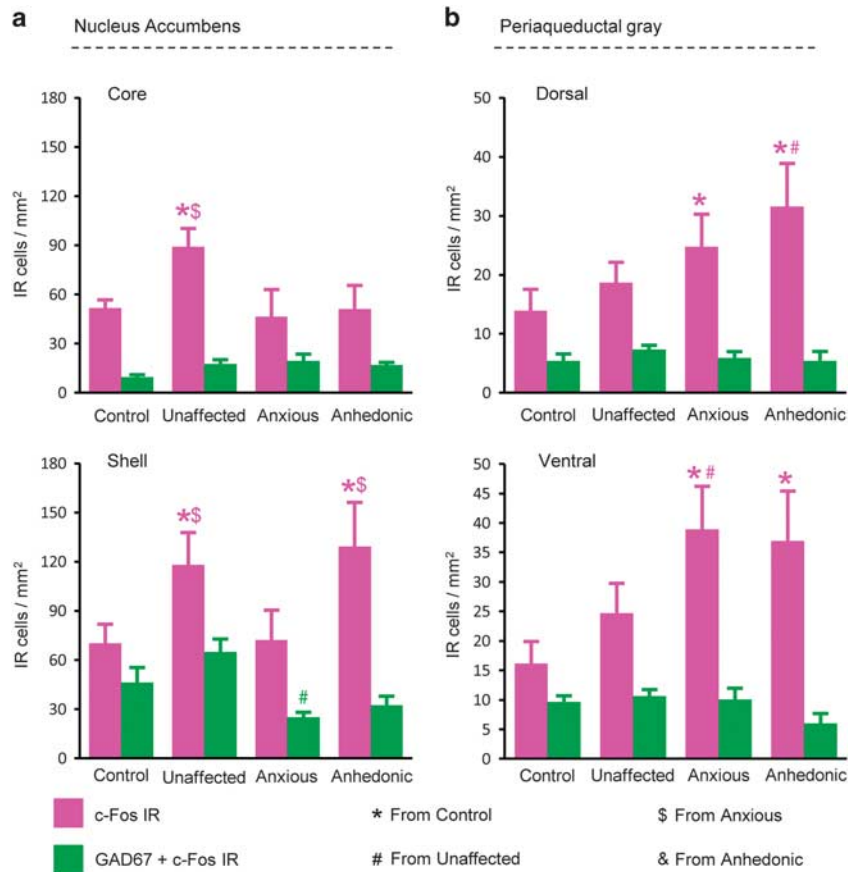


Figure 4. Differential activation in the periaqueductal gray and nucleus accumbens (NA) in the different phenotypes of underwater trauma (UWT) and control rats. **(a)** Differences in activation (total c-Fos-expressing cells) and activation of inhibition (dual-labeled (DL) cells count) in the NA layers between the different phenotypes of UWT and control rats. **(b)** Differences in activation and activation of inhibition in the dorsal and ventral regions of the periaqueductal gray between the different phenotypes of UWT and control rats. Bars represent the groups mean \pm s.e.m. Significant Bonferroni *post-hoc* results with $P < 0.05$ are flagged as: *different from control; #different from unaffected; \$different from affected anxious; and &different from affected anhedonic. IR, immunoreactive.

subtypes of affected style. Immunohistochemical assessment of c-Fos expression as a marker of cellular activity and GAD67 dual-labeling as a marker for active inhibitory GABAergic cells was used to calculate regional activation (total c-Fos-expressing cells) and activation of inhibition (total GAD67-labeled cells expressing c-Fos; Figure 2b). The results of this assessment indicated that the classification of rats to different affected behavioral style has functional correlates of activation and inhibition in the limbic system. One-way ANOVAs found significant effects between the response subtypes in UWT and control rats in the prelimbic (PL; c-Fos: $F_{(3,38)} = 5.4, P = 0.003$; dual-labeled (DL): $F_{(3,38)} = 5.4, P < 0.001$) and infralimbic (IL; c-Fos: $F_{(3,38)} = 8.9, P < 0.001$; DL: $F_{(3,38)} = 4.7, P = 0.007$) divisions of the mPFC (Figure 2c), central (CeA; c-Fos: $F_{(3,38)} = 16.3, P < 0.001$; DL: $F_{(3,38)} = 2.6, P = 0.064$) and basolateral (BLA; c-Fos: $F_{(3,38)} = 6, P = 0.002$; DL: $F_{(3,38)} = 6.8, P = 0.001$) nuclei of the amygdala (Figure 2b). As can be seen in Figure 3, significant group effects were found in the dorsal hippocampus cornu ammonis 3 (dCA3; c-Fos: $F_{(3,38)} = 8.5, P < 0.001$; DL: $F_{(3,38)} = 2.9, P = 0.050$) and dentate gyrus (DG) (dDG; c-Fos: $F_{(3,38)} = 3.8, P = 0.019$; DL: $F_{(3,38)} = 5.9, P = 0.002$) layers (Figure 3a), as well as in its ventral cornu ammonis 1 (vCA1; c-Fos: $F_{(3,38)} = 5.9, P = 0.002$; DL: $F_{(3,37)} = 13.4, P < 0.001$), CA3 (vCA3; c-Fos: $F_{(3,37)} = 5.5, P = 0.003$; DL: $F_{(3,37)} < 1$) and DG (vDG; c-Fos: $F_{(3,38)} = 15.6, P < 0.001$; DL: $F_{(3,38)} = 6.9, P = 0.001$) layers (Figure 3b). Finally, significant effects between the subtypes of response and control rats were found in the NA core (NAC; c-Fos: $F_{(3,38)} = 5.9, P = 0.002$; DL: $F_{(3,38)} = 1.9, P = 0.148$) and shell (NAS; c-Fos: $F_{(3,38)} = 8.1, P < 0.001$; DL:

$F_{(3,38)} = 6.8, P = 0.001$) (Figure 4a), as well as in the PAG's dorsal (dPAG; c-Fos: $F_{(3,38)} = 9.6, P < 0.001$; DL: $F_{(3,38)} < 1$) and ventral (vPAG; c-Fos: $F_{(3,38)} = 15.1, P < 0.001$; DL: $F_{(3,38)} = 1.2, P = 0.332$) divisions (Figure 4b).

Limbic network patterns of activity shift in accordance with the behavioral response

In order to test the hypothesized contribution of differential modulation within the mPFC–hippocampus–amygdala circuit to the diversity of stress response,⁹ we implemented further analyses to characterize the network pattern of activity in each behavioral subtype. At first, we evaluated whether the defined types of responses are reflected in the ratio of activity within the different regions. For this, the count of activated non-GABAergic cells was divided by the count of activated GABAergic cells (that is, DL count). One-way ANOVAs with Bonferroni *post-hoc* correction confirmed that nearly all intra-regional ratios were significantly affected by the type of response (detailed comparisons can be found in Supplementary Table S1). We then depicted the prominent effects at the network level. Every intra-regional ratio that significantly differed from the mean ratio of control was marked as either higher excitation or higher inhibition to present the dominant state of activity within the region. As illustrated in Figure 5, this has revealed a prominent shift in the intra-regional ratio of activity of the affected phenotypes. Although the pattern of unaffected rats was rather similar to control (Figure 5a), the

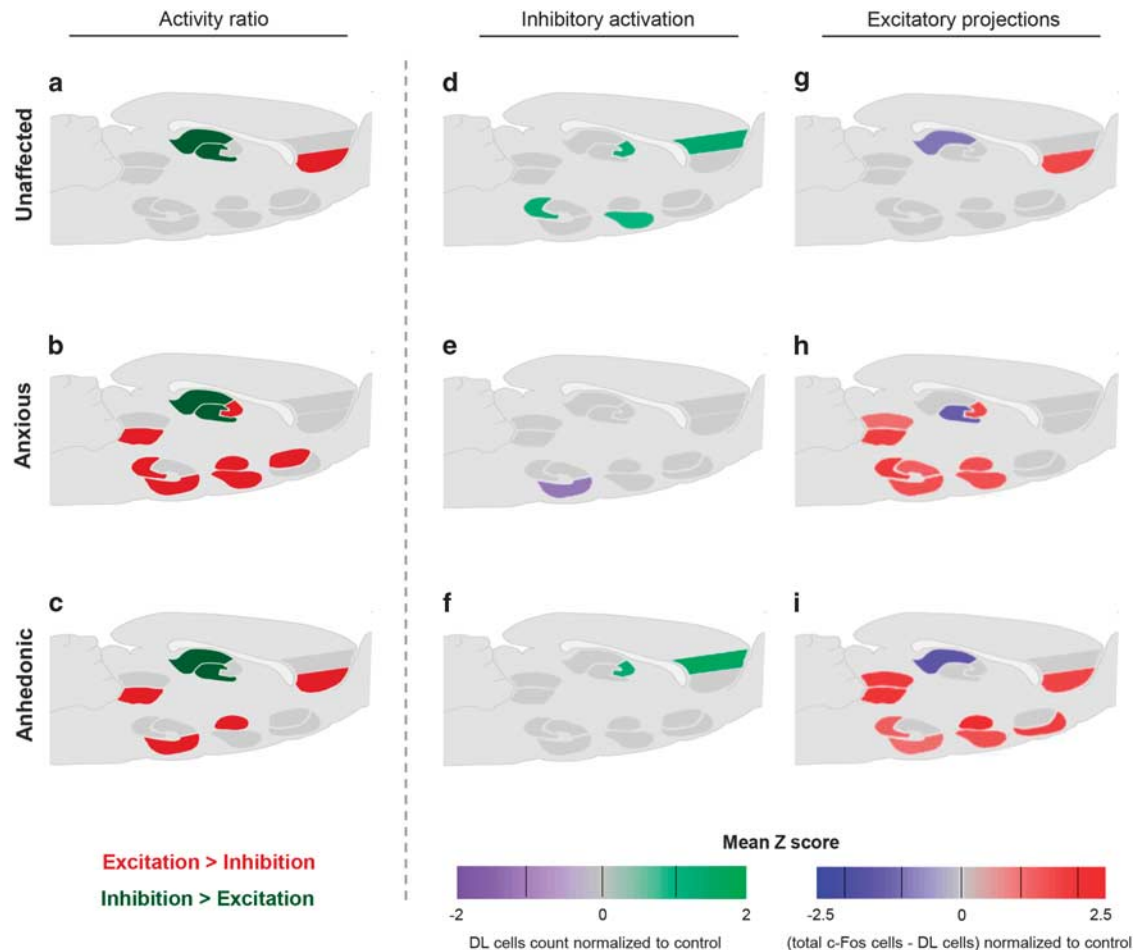


Figure 5. Limbic patterns of activity shift in accordance with the behavioral response of underwater trauma (UWT) rats. Left panel: Significant effects for the type of response on intra-regional ratio of activity (non-GABAergic c-Fos count/dual-labeled (DL) count; See Supplementary Table S1 for detailed comparisons). Right panels: Significant alterations in the degree of inhibitory activation (DL count normalized to control) and excitatory projections ((non-GABAergic c-Fos count – DL count) normalized to control; See Supplementary Table S2 for detailed comparisons). (a) Unaffected rats, which went through the UWT but did not have an anxious-like response during the context re-exposure, show intra-regional ratio of activity that is rather similar to control (gray). In contrast, the affected anxious (b) and the co-morbid anhedonic rats (c) show intra-regional ratios of dominant excitation in the amygdala, ventral hippocampus and ventral periaqueductal gray (PAG). (d) The unaffected rats show an increase in the degree of inhibitory activation in the prelimbic cortex (PL), basolateral amygdala, dorsal cornu ammonis 3 (dCA3) and ventral dentate gyrus. In contrast to that, the affected anxious rats (e) show a decrease in the degree of inhibitory activation only in the ventral cornu ammonis 1, while the co-morbid anhedonic rats (f) show a decrease in the degree of inhibitory activation only in the PL and dCA3. (g) The unaffected rats show an increase in the degree of excitation in the infralimbic cortex. In contrast to that, the affected anxious rats (h) show an increase in the degree of excitation in the amygdala, ventral hippocampus and PAG. (i) The co-morbid anhedonic rats show an increase in the degree of excitation in the amygdala, ventral hippocampus, PAG and nucleus accumbens shell.

affected phenotype patterns involved intra-regional ratios of dominant excitation in the amygdala, ventral hippocampus and PAG. Furthermore, there were also differences between the two affected phenotypes; in the anxious phenotype, dominant excitation was evident in the dorsal CA3, ventral CA1, DG, PAG and both nuclei of the amygdala and NAC (Figure 5b). In the anhedonic phenotype, dominant excitation was evident in the ventral CA1 and PAG, CeA nuclei and IL (Figure 5c).

Next, we depicted the alterations in the degree of inhibitory and excitatory activation at the network level. For inhibitory activation, every DL count that significantly differed from control was normalized to the relevant control's group mean (that is, (individual DL count – control mean DL count)/overall s.d.). As shown in Figure 5d, the unaffected type of response was associated with an increase, compared with control, of inhibitory activation in the PL, BLA, dCA3 and vDG. In contrast, in the affected phenotypes no substantial inhibitory activation pattern

alterations were found. The anxious type of response was associated with a decrease in inhibition only in the vCA1 (Figure 5e), while the co-morbid anhedonic type was found to be associated with an increased inhibition in the PL and dCA3 (Figure 5f). For the degree of excitatory activation, we first compared the counts of activated non-GABAergic cells (that is, excitatory activation) in the different regions between the different groups. One-way ANOVAs with Bonferroni *post-hoc* correction revealed prominent group effects for the degree of excitatory activation as nearly all regions were significantly affected by the type of behavioral response, thus confirming the relevance of the behavioral profiling approach we have employed (detailed comparisons can be found in Supplementary Table S2). We then used linear regressions to evaluate if the degree of this excitatory activation measure relates to fear memory retrieval and assessed its predictive power in comparison to the initial measure of overall activation (total c-Fos). As it was previously suggested

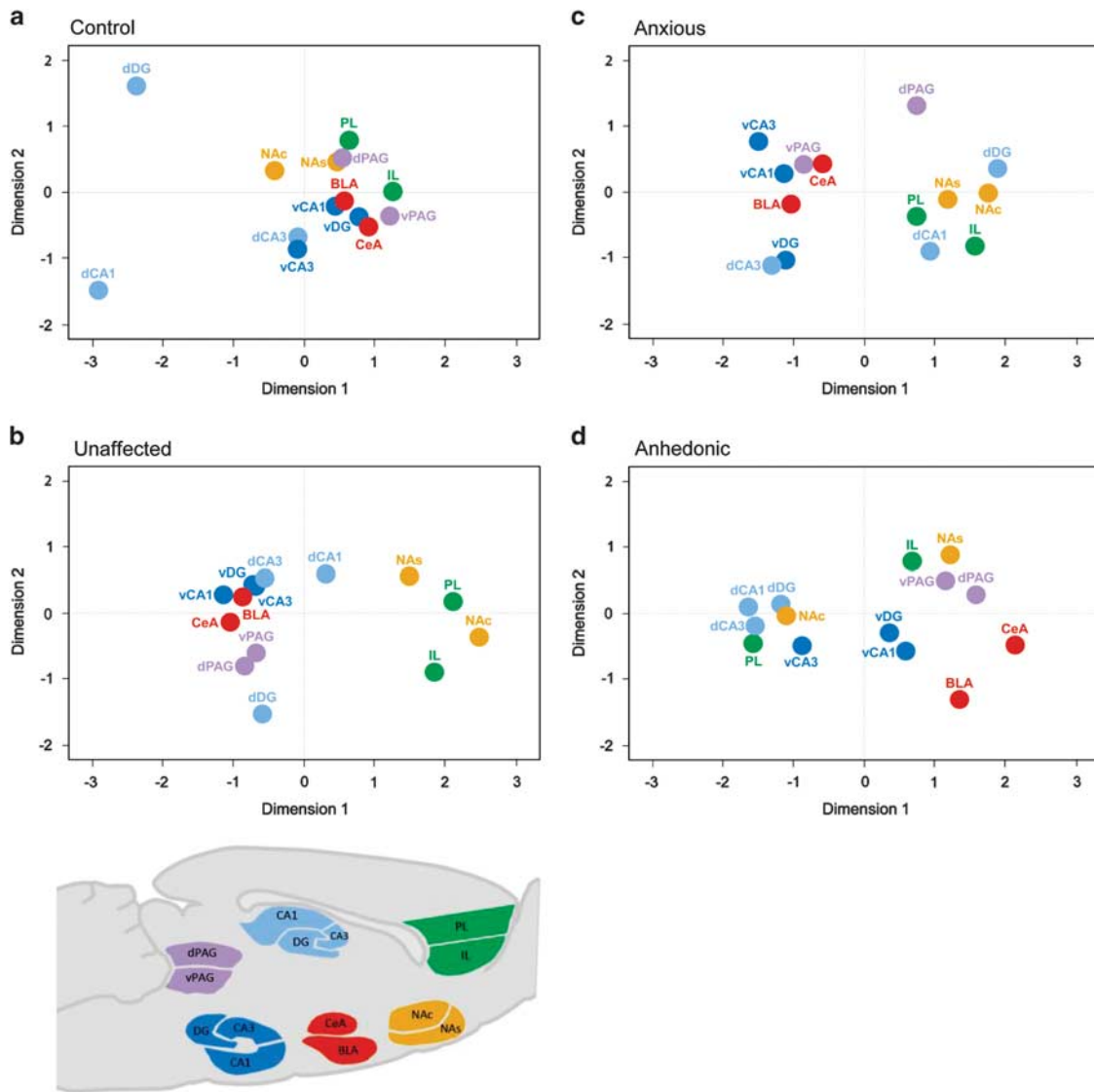


Figure 6. Multidimensional scaling reveals different patterns of co-activity in the limbic network of trauma-exposed rats. Coordinated co-activity is represented by relative distance. Points that are close to each other represent simultaneous similarities in regional excitation. The descriptive matrices indicate that relative to (a) control ($n = 11$, Stress = 0.070, R-square (RSQ) = 0.990), the exposure to a contextual reminder of UWT associates with a disseminated network. (b) Unaffected ($n = 14$, Stress = 0.044, RSQ = 0.993). (c) Anxious ($n = 12$, Stress = 0.079, RSQ = 0.971). (d) Anhedonic ($n = 5$, Stress = 0.068, RSQ = 0.979). BLA, basolateral amygdala; CeA, central amygdala; DG, dentate gyrus; d/vCA1, dorsal/ventral cornus ammonis 1; d/vCA3, dorsal/ventral cornus ammonis 3; d/vDG, dorsal/ventral dentate gyrus; d/vPAG, dorsal/ventral periaqueductal gray; IL, infralimbic cortex; NAc, nucleus accumbens core; NAs, nucleus accumbens shell; PL, peririmbic cortex.

that the expression of fear behavior, during the retrieval of a contextual fear memory, is mediated by the PL,^{10,11,25} BLA^{13,26,30} and ventral DG,^{24,34,35} we evaluated the relation between this circuitry and the degree of freezing during the WAZM re-exposure. These analyses revealed that, in comparison to the initial measure for overall activation, the excitatory activation relates more directly to the specific expression of learned fear (Supplementary Table S3). Moreover, the excitatory activation model linked the strength of the relationship between PL–BLA–vDG circuit activity and degree of freezing to the characteristics of the groups. Thus, in the control rats, for which the context was not paired with any significant stimulus, the PL–BLA–vDG excitation had no significant outcome ($F < 1$), with the circuit's activity predicting < 7% of the variance in their freezing. In contrast, in the UWT rats, for which the context was paired with an uncontrollable near-drowning experience, the strength of the relationship shifted in an ordinal manner. In the unaffected group, the model implied for a weak,

insignificant relation ($F < 1$), with their PL–BLA–vDG excitation predicting 21% of the variance in their freezing. In the anxious phenotype, the PL–BLA–vDG excitation had a strong significant effect ($F = 5.1$, $P = 0.03$), predicting > 65% of the variance in their freezing. Interestingly, for the anhedonic phenotype group, high predictive power was found for their model (accounting for 89% of the variance in their freezing), though given the small size of this group it did not reach a significant level ($F = 2.5$, $P = 0.4$). To more visually be able to appreciate the network-level effect, we then illustrated the alterations in the patterns of excitation (Figures 5g–i). For this analysis, only regional excitations that significantly differed from the control's group mean were used (Supplementary Table S2). Relevant degrees of excitation were normalized to the control group mean (that is, (individual degrees of excitation – control mean degrees of excitation)/overall s.d.) and clustered to exemplify major alterations in the patterns of excitatory activity. In contrast to the patterns of inhibitory

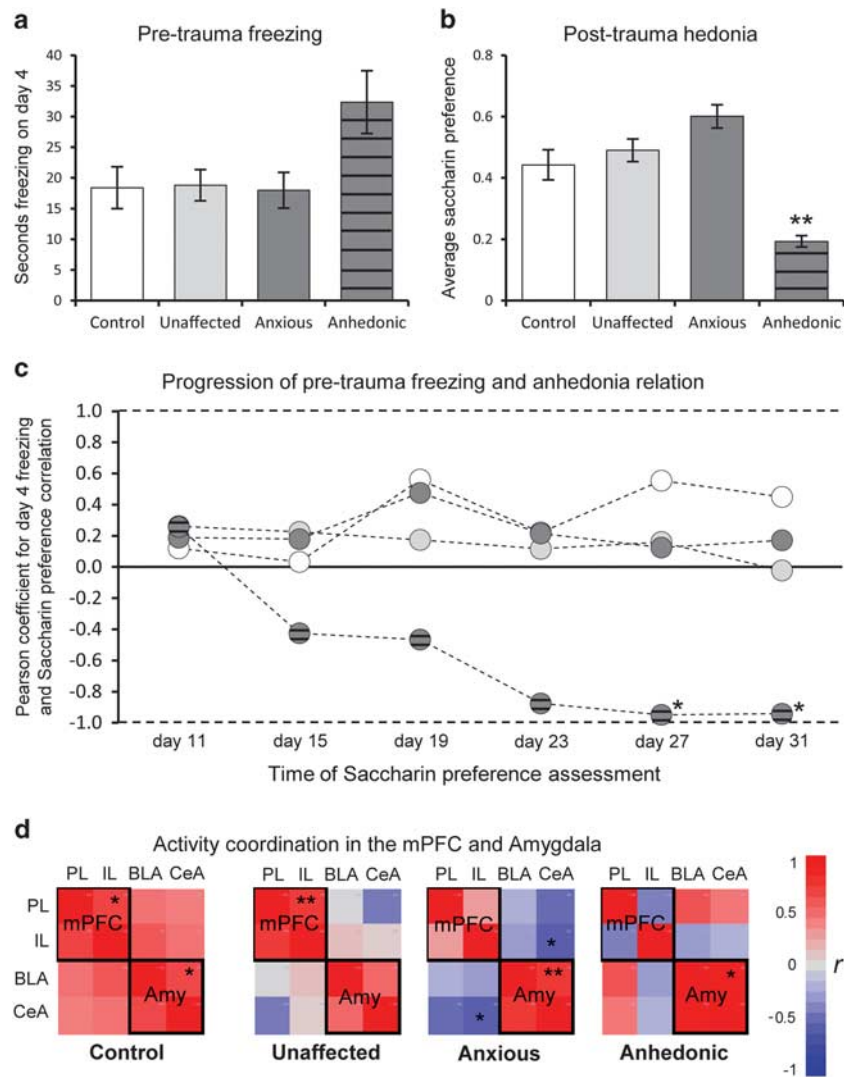


Figure 7. Pretrauma anxiety relates to the posttrauma progression of anhedonic behavior only in the co-morbid anhedonic phenotype. This is in accordance with the predictions of the ‘high anxiety trait to posttraumatic depression’ model of Sandi and Richter-Levin.²⁹ (a) Pretrauma anxiety-like behavior as measured by freezing during the context habituation on day 4 ($F_{(3,41)} = 2.5$, $P = 0.072$). (b) Posttrauma hedonia as measured by the average preference for saccharin during the 4 weeks interval. Bars represent the groups’ mean \pm s.e.m. Significant Bonferroni post-hoc results with $P < 0.01$ are flagged as: **different from control, unaffected and affected anxious. (c) The correlation between pretrauma freezing and posttrauma saccharin preference assessments (see also Supplementary Figure S3e). (d) The inter-relations within the medial prefrontal cortex (mPFC) and amygdala (Amy), as measured by the degree of excitation in their sub-regions in the different groups. Two-tailed Pearson tests, * $P < 0.05$; ** $P < 0.01$. BLA, basolateral amygdala; CeA, central amygdala; IL, infralimbic cortex; PL, perilimbic cortex.

activation, this has revealed a prominent shift in the excitation degree patterns of the affected phenotypes (Figures 5g–i). Although the pattern of unaffected rats was rather similar to control (Figure 5g), the affected phenotype patterns involved a general increase in the degree of excitation in the amygdala, ventral hippocampus and PAG. Furthermore, differences could be found between the affected phenotypes, such that in the anxious phenotype a distinct increase was evident in both ventral and dorsal CA3, accompanied with a distinct decrease in dDG excitation (Figure 5h), whereas in the anhedonic phenotype a distinct increase was found in the NAs excitation (Figure 5i).

At the final step, we explored the degree of coordinated co-activity within the patterns of excitation of the different exposed subtypes and control rats. We used MDS to model the network level of co-activity and illustrate the possible patterns of simultaneous excitations in all regions together. The primary outcome of this descriptive analysis is visualized through a two-

dimension distance matrix, in which the data, that is, excitation of the sub-regions, are represented as points. These points are arranged in such a way that their distances correspond to the overall similarities in their pattern of excitation.³³ Coordinated co-activity between regions is represented by points that are close to each other, whereas disorganized co-activity is represented by points that are far apart.

Separately conducted for each group, the MDS analyses produced utterly different matrices of co-activity within the network for each group subtype. As shown in Figure 6, an exposure to a contextual reminder associated with a disseminating shift in the network coordination among all UWT rats, including in the exposed, unaffected group. In the affected anxious rats’ group, the dorsal CA1 and DG were grouped with the mPFC, NA and dorsal PAG, while the ventral regions of their hippocampus were grouped with the ventral PAG and amygdala (Figure 6c). Such a pattern is in line with the hypothesized effects of stress on dorsal

and ventral hippocampus functions^{34,35} and our previous report of ventral hippocampus and amygdala coordination during the recollection of an UWT experience.²⁴

Differing from the pure anxious phenotype, the anhedonic rats' matrix revealed a unique separation within the network, involving a distinct distancing between the amygdala and the rest of the limbic system (Figure 6d). In addition, the anhedonic phenotype co-activity pattern was found to be associated with an exclusive separation between the PL and IL divisions of the mPFC (Figure 6d). These characteristics seem to follow the 'high anxiety trait to depression' model suggested by Sandi and Richter-Levin.²⁹ According to this model, among individuals with high anxiety trait an enhanced amygdala reactivity to stress exposure produces long-term disruptions in mPFC regulation and a negative mood bias. In time, this progressive mPFC dysregulation can synergize with the trait for heightened fear responses and gradually result in posttraumatic depression. To evaluate the validity of these predictions, we conducted a series of tests to compare pretrauma anxious-like behavior between the groups and to assess its relation to posttrauma anhedonia. Retrospective measures of freezing during the day 4 context habituation were used to assess basic, pre-trauma, fear responses. One-way ANOVA showed that anhedonic rats had a mildly significant trend of enhanced freezing behavior during the pretrauma habituation to the WAZM ($F_{(3,41)}=2.5$, $P=0.072$; Figure 7a). Pearson correlation tests were then used to assess the relation between this basic fear response and the repeated assessments of saccharin consumption. In accordance with the predictions of Sandi and Richter-Levin's model,²⁹ we found that pretrauma freezing correlated with posttrauma saccharin preference only among the anhedonic rats. As shown in Figure 7c, this effect showed development over time, as the correlation coefficients evolved over the 1-month interval, nearly reaching linearity for the final CSP assessments (day 27: $r=-0.95$, $P=0.014$; day 31: $r=-0.94$, $P=0.017$). Finally, Pearson correlation tests were used to assess the inter-relations within the degree of excitation of the mPFC and amygdala sub-regions in the different groups. As depicted in Figure 7d, significant direct correlations between the PL and IL of the mPFC were found only in the control ($r=0.7$, $P<0.05$) and unaffected ($r=0.75$, $P<0.01$) rats. No significant correlations were found between the PL and IL of the mPFC among the anxious ($r=0.28$, $P=0.37$) or anhedonic ($r=-0.42$, $P=0.48$) phenotypes. With regard to the amygdala, significant direct correlations between the BLA and CeA were found among the control rats ($r=0.67$, $P<0.05$) and among the affected anxious ($r=0.77$, $P<0.01$) and anhedonic ($r=0.93$, $P<0.05$) phenotypes, but not among the unaffected rats ($r=0.52$, $P=0.054$) (Figure 7d).

DISCUSSION

It was previously shown that a single episode of acute underwater stress increases anxious-like behaviors and differentially affects the dorsal and ventral layers of the hippocampus, both at the short²⁴ and long term^{36,37} after trauma exposure. By introducing an individual profiling approach, which models the diagnostic criteria of PTSD in rats,^{16,17,38} to underwater stress-exposed rat population, we have identified an affected, extremely anxious, sub-group with an occurrence rate of 53%. This prevalence highly resembles the probability for males to meet full PTSD diagnosis following severe trauma exposure, as combat or rape (~40–60%).³⁹ Furthermore, combining both anxious-like and anhedonic behavioral assessments enabled us to discern between different subtypes of reaction style and specify two phenotypes of affected rats, an utterly fear-based anxious phenotype and a co-morbid anhedonic phenotype. This diversity within affected rats' responses is similar to the psychiatric acknowledged symptom range of more anxious—fear based—or more anhedonic—

dysphoric responses—to trauma,¹ as well as phenotype variety in PTSD patients.¹⁴

Disregarding the pattern of different symptoms, by grouping of all patients in PTSD research, has been suggested to limit the understanding of posttraumatic psychopathology and its neural correlates.⁹ The significant differences we found between the different subtypes of stress response, and control rats, in activation and inhibition of different regions further validates the individual profiling approach and the functionality of its behavioral classifications.

Combining this classification with the characterization of the network ratio of excitation revealed a fundamental difference between the activity patterns of the unaffected rats and the affected anxious or anhedonic phenotypes, thus, allowing us to characterize the neural systems that correlate with each affected phenotype. Among all affected rats, a significant increase in the degree of excitation was observed in the amygdala, ventral hippocampus and PAG. This is in line with previous suggestions regarding stress effects on the ventral hippocampus^{34,35} and its involvement in long-term anxious reactions to UWT.^{36,37} Nevertheless, notable excitations, differentiating between the more anxious and anhedonic phenotypes, were observed in the dorsal hippocampus and NA. The clear anxious phenotype was associated with a distinct excitatory activity in the dorsal CA3 and NAc (Figure 5b). These findings of distinctive alterations in maps of brain activity between the behaviorally categorized phenotypes lands important support to the functional significance of the behavioral profiling approach.

It has long been suggested that the attention of research regarding the aftermath of stress exposure should be shifted from focusing on the effects of stress on specific brain regions to a more system-level approach that emphasizes possible modification of inter-region interactions.^{6,9,10,12,14,26,29,34,40} In line with this perspective, we found that an exposure to a contextual reminder 1 month after UWT was accompanied by a disperse shift in the pattern of co-activity within the limbic network (Figures 6b–d). Interestingly, again, a number of notable differences were observed between the descriptive matrices of the affected phenotypes. In the anxious rats, who showed an increased amygdala and ventral hippocampus excitation (Figures 5b and h), dorsal hippocampus activity coordinated with the mPFC and NA, yet desynchronized with the ventral hippocampus. In contrast, ventral hippocampus activity was coordinated with amygdala activity (Figure 6c). This is consistent with our previous report of a specific pattern of neural activation during the recollection of UWT experience, involving ventral hippocampus and amygdala synchronization.²⁴ With regard to psychiatric theories of PTSD phenotypes, such a disorganized pattern of co-activity partially corresponds to the suggested role of emotion under-modulation in the re-experiencing, more anxious phenotype of PTSD.⁹

It is important to note that the co-morbid group, classified as anhedonic, was rather small ($n=5$). Therefore, any conclusions inferred from its data should be considered with caution. Nevertheless, the occurrence rate of this condition among the overall affected anxious rats in our study was 27.8% (5/18). This is similar to the reported rate of co-morbid major depression occurrence (23%) among PTSD patients.⁴¹ As in the anxious phenotype, the anhedonic rats showed an increased degree of amygdala and ventral hippocampus excitation. However, this co-morbid condition was additionally associated with an increase of excitation in the IL (Figures 5c and f), as was also found in the unaffected group (Figures 5a and g). This is in line with human imaging data, indicating that following trauma exposure both unaffected individuals and PTSD patients with co-morbid major depression respond to trauma reminders with greater mPFC activation in comparison to clear PTSD patients.⁴² These anhedonic rats also showed a distinctive and prominent increased degree of excitation in the NAs, a key brain region for hedonic

behavior.²⁸ Furthermore, only among this group a unique pattern of intra-regional disorganization was found, involving disordered co-activity between the sub-regions of both the mPFC and the NA. Although their PL activity coordinated with the dorsal hippocampus and NAc, their IL activity coordinated with the PAG and NAs (Figure 6d). Although purely descriptive, these alterations are in line with a recent suggestion regarding the role of stress-induced impairments in the mPFC and its limbic projections as mediators of stress susceptibility. According to this proposition, mPFC–BLA projections mediate stress-induced anxiety symptoms, whereas mPFC–NAc projections mediate the depression-like effects of social stress.⁴³ In addition to uncoordinated mPFC activity, the anhedonic phenotype co-activity matrix revealed a distinct separation between their hyper-excited amygdala and the rest of the network (Figure 6d). Such abnormal co-activity corresponds well with the cortico-amygdala feedback deficiencies suggested to mediate dysphoric emotions and symptoms of depression.⁴³ Furthermore, such a pattern seems to follow the 'high anxiety trait to depression' hypothesis of Sandi and Richter-Levin.²⁹ According to this neurocognitive model for posttraumatic depression pathogenesis, among high anxiety trait individuals a sensitized amygdala and its enhanced reactivity to stress exposure can fundamentally disrupt mPFC functions. In turn, this will impair the mPFC effectiveness in restraining fear reactions and incite psychophysiological alterations at the base of emotion processing. Sandi and Richter-Levin's model predicts that such a progressive spiral of disrupted regulation will gradually synergize the heightened fear memory with a negative mood bias, to result in long-term depressive dysfunction. Indeed, the anhedonic phenotype was found to be associated with a segregated mPFC inner-activity trend (Figures 6c and 7d). In line with the model's predictions, the anhedonic phenotype showed a trend for enhanced reflexive fear behavior before the UWT exposure (Figure 7a), as well as a prominent decrease in the averaged preference for saccharin (Figure 7b), which gradually became evident after the UWT exposure (see Supplementary Figure S3e). Strikingly, only among these rats did the individual trait for fear response, before the UWT, related to the development of anhedonic behavior over time, accurately predicting its degree 1 month after the exposure (Figure 7c).

It was recently suggested that the diversity in behavioral responses, often observed in studies using rodent models of PTSD, should be directly addressed in order to better understand the pathophysiology of this disorder.⁴⁴ The current data strongly support this notion and demonstrate how an individual profiling approach can be used for discerning affected sub-groups in a rodent population. The current behavioral profiling approach adds to previous classifications both in referring to the behavior of the control population as the norm, as is the practice in human diagnosis, and by differentiating between different profiles of affected individuals. Importantly, combining this behavioral profiling with a network-level analysis uncovered distinct micro-anatomical correlates and co-activity patterns within the limbic systems of the different affected phenotypes.

It is important to note that the neuroanatomical correlates we found within the limbic system of the different phenotypes relayed on the assessment of c-Fos expression in non-GABAergic and GABAergic cells. As it was previously suggested that not all kinds of neurons may show c-Fos induction upon activation,⁴⁵ future studies of abnormal stress responses in rodents should consider the use of additional biochemical markers for different types of cells.

In recent studies,^{31,44} behavioral categorization has already been employed to search for possible neural candidates that contribute to individual differences in stress response. For example, glucocorticoid receptor signaling in the hippocampus and amygdala was found to be significantly associated with extreme anxiety symptoms.⁴⁴ The current study did not examine specific neural targets and their association with exposure-related

individual differences. However, the differences in maps of activation between exposed-unaffected individuals, anxious, fear-based individuals and co-morbid, fear-anhedonic individuals indicates that future studies aiming to reveal the neural base for individual differences in stress vulnerability, and stress response, would benefit from employing a profiling analysis as proposed here. Identifying vulnerable individuals, and different affected styles among stress exposed rodents, can promote the development of more personalized interventions that target specific behavioral and neuronal connectivity patterns. This can direct future translational research and help bridging the gap between rodent's behavior and human psychopathology.

CONFLICT OF INTEREST

The authors declare no conflict of interest.

ACKNOWLEDGMENTS

This work was supported by a DOD award number W81XWH-11-2-0111 to GR-L.

REFERENCES

- 1 American Psychiatric Association. *Diagnostic and Statistical Manual of Mental Disorders*, 5th (edn). American Psychiatric Publishing: Arlington, VA, USA, 2013.
- 2 Dias BG, Goodman JV, Ahluwalia R, Easton AE, Andero R, Ressler KA. Amygdala-dependent fear memory consolidation via miR-34a and Notch signaling. *Neuron* 2014; **83**: 906–918.
- 3 Nader K, Hardt O, Lanius RA. Memory as a new therapeutic target. *Dialogues Clin Neurosci* 2013; **15**: 475–486.
- 4 Andero R, Dias BG, Ressler KJ. A role for Tac2, NkB, and Nk3 receptor in normal and dysregulated fear memory consolidation. *Neuron* 2014; **83**: 444–454.
- 5 Otis JM, Werner CT, Mueller D. Noradrenergic regulation of fear and drug-associated memory reconsolidation. *Neuropsychopharmacology* 2014; **40**: 793–803.
- 6 Lanius RA, Williamson PC, Densmore M, Boksman K, Neufeld RW, Gati JS et al. The nature of traumatic memories: a 4-T fMRI functional connectivity analysis. *Am J Psychiatry* 2004; **161**: 36–44.
- 7 Spiegel D. Trauma, dissociation, and memory. *Ann NY Acad Sci* 1997; **821**: 225–237.
- 8 van der Kolk B. Posttraumatic stress disorder and the nature of trauma. *Dialogues Clin Neurosci* 2000; **2**: 7–22.
- 9 Lanius RA, Vermetten E, Loewenstein RJ, Brand B, Schmahl C, Bremner JD et al. Emotion modulation in PTSD: clinical and neurobiological evidence for a dissociative subtype. *Am J Psychiatry* 2010; **167**: 640–647.
- 10 Knapaska E, Macias M, Mikosz M, Nowak A, Owczarek D, Wawrzyniak M et al. Functional anatomy of neural circuits regulating fear and extinction. *Proc Natl Acad Sci USA* 2012; **109**: 17093–17098.
- 11 Maren S, Phan KL, Liberzon I. The contextual brain: implications for fear conditioning, extinction and psychopathology. *Nat Rev Neurosci* 2013; **14**: 417–428.
- 12 Admon R, Milad MR, Hendler T. A causal model of post-traumatic stress disorder: disentangling predisposed from acquired neural abnormalities. *Trends Cogn Sci* 2013; **17**: 337–347.
- 13 Sotres-Bayon F, Sierra-Mercado D, Pardilla-Delgado E, Quirk GJ. Gating of fear in prelimbic cortex by hippocampal and amygdala inputs. *Neuron* 2012; **76**: 804–812.
- 14 Lanius RA, Brand B, Vermetten E, Frewen PA, Spiegel D. The dissociative subtype of posttraumatic stress disorder: rationale, clinical and neurobiological evidence, and implications. *Depress Anxiety* 2012; **29**: 701–708.
- 15 Pitman RK, Rasmusson AM, Koenen KC, Shin LM, Orr SP, Gilbertson MW et al. Biological studies of post-traumatic stress disorder. *Nat Rev Neurosci* 2012; **13**: 769–787.
- 16 Cohen H, Zohar J, Matar MA, Zeev K, Loewenthal U, Richter-Levin G. Setting apart the affected: the use of behavioral criteria in animal models of post traumatic stress disorder. *Neuropsychopharmacology* 2004; **29**: 1962–1970.
- 17 Horowitz O, Tsoory MM, Hall J, Jacobson-Pick S, Richter-Levin G. Post-weaning to pre-pubertal ('juvenile') stress: a model of induced predisposition to stress-related disorders. *Neuroendocrinology* 2012; **95**: 56–64.
- 18 Cohen H, Matar MA, Zohar J. Maintaining the clinical relevance of animal models in translational studies of post-traumatic stress disorder. *ILAR J* 2014; **55**: 233–245.
- 19 Matar MA, Zohar J, Cohen H. Translationally relevant modeling of PTSD in rodents. *Cell Tissue Res* 2013; **354**: 127–139.
- 20 Richter-Levin G. Acute and long-term behavioral correlates of underwater trauma—potential relevance to stress and post-stress syndromes. *Psychiatry Res* 1998; **79**: 73–83.

- 21 Cohen H, Liberzon I, Richter-Levin G. Exposure to extreme stress impairs contextual odor discrimination in an animal model of PTSD. *Int J Neuropsychopharmacol* 2009; **12**: 291–303.
- 22 Moore NL, Gauchan S, Genovese RF. Differential severity of anxiogenic effects resulting from a brief swim or underwater trauma in adolescent male rats. *Pharmacol Biochem Behav* 2012; **102**: 264–268.
- 23 Ardi Z, Ritov G, Lucas M, Richter-Levin G. The effects of a reminder of underwater trauma on behaviour and memory-related mechanisms in the rat dentate gyrus. *Int J Neuropsychopharmacol* 2014; **17**: 571–580.
- 24 Ritov G, Ardi Z, Richter-Levin G. Differential activation of amygdala, dorsal and ventral hippocampus following an exposure to a reminder of underwater trauma. *Front Behav Neurosci* 2014; **8**: 18.
- 25 Furlong TM, Cole S, Hamlin AS, McNally GP. The role of prefrontal cortex in predictive fear learning. *Behav Neurosci* 2010; **124**: 574–586.
- 26 Kim EJ, Horovitz O, Pellman BA, Tan LM, Li Q, Richter-Levin G *et al*. Dorsal periaqueductal gray-amygdala pathway conveys both innate and learned fear responses in rats. *Proc Natl Acad Sci USA* 2013; **110**: 14795–14800.
- 27 Badrinarayan A, Wescott SA, Vander Weele CM, Saunders BT, Couturier BE, Maren S *et al*. Aversive stimuli differentially modulate real-time dopamine transmission dynamics within the nucleus accumbens core and shell. *J Neurosci* 2012; **32**: 15779–15790.
- 28 Berridge KC, Kringelbach ML. Neuroscience of affect: brain mechanisms of pleasure and displeasure. *Curr Opin Neurobiol* 2013; **23**: 294–303.
- 29 Sandi C, Richter-Levin G. From high anxiety trait to depression: a neurocognitive hypothesis. *Trends Neurosci* 2009; **32**: 312–320.
- 30 Ritov G, Richter-Levin G. Water associated zero maze: a novel rat model for long term traumatic re-experiencing. *Front Behav Neurosci* 2014; **8**: 1.
- 31 Cohen S, Vainer E, Matar MA, Kozlovsky N, Kaplan Z, Zohar J *et al*. Diurnal fluctuations in HPA and neuropeptide Y-ergic systems underlie differences in vulnerability to traumatic stress responses at different zeitgeber times. *Neuropsychopharmacology* 2015; **40**: 774–790.
- 32 Cooke T, Wallraven C, Bulthoff HH. Multidimensional scaling analysis of haptic exploratory procedures. *ACM Trans Appl Percept* 2010; **7**: 1.
- 33 Wickelmaier F. An Introduction to MDS. Reports from the Sound Quality Research Unit (SQRU) 7, (2003). Available at <http://homepages.unituebingen.de/florian.wickelmaier/pubs/Wickelmaier2003SQRU.pdf>.
- 34 Segal M, Richter-Levin G, Maggio N. Stress-induced dynamic routing of hippocampal connectivity: a hypothesis. *Hippocampus* 2010; **20**: 1332–1338.
- 35 Maggio N, Segal M. Cellular basis of a rapid effect of mineralocorticosteroid receptors activation on LTP in ventral hippocampal slices. *Hippocampus* 2012; **22**: 267–275.
- 36 Sood R, Ritov G, Richter-Levin G, Barki-Harrington L. Selective increase in the association of the Beta 2 adrenergic receptor, Beta Arrestin-1 and p53 with Mdm2 in the ventral hippocampus one month after underwater trauma. *Behav Brain Res* 2013; **240**: 26–28.
- 37 Sood R, Ritov G, Boltyansky B, Spector-Chotiner A, Richter-Levin G, Barki-Harrington L. Underwater trauma causes a long-term specific increase in the expression of cyclooxygenase-2 in the ventral CA1 of the hippocampus. *Psychoneuroendocrinology* 2014; **49**: 62–68.
- 38 Horovitz O, Tsoory MM, Yovell Y, Richter-Levin G. A rat model of pre-puberty (juvenile) stress-induced predisposition to stress-related disorders: sex similarities and sex differences in effects and symptoms. *World J Biol Psychiatry* 2014; **15**: 36–48.
- 39 Nemeroff CB, Bremner JD, Foa EB, Mayberg HS, North CS, Stein MB. Posttraumatic stress disorder: a state-of-the-science review. *J Psychiatr Res* 2006; **40**: 1–21.
- 40 Maroun M, Richter-Levin G. Exposure to acute stress blocks the induction of long-term potentiation of the amygdala-prefrontal cortex pathway in vivo. *J Neurosci* 2003; **23**: 4406–4409.
- 41 Conner KR, Bossarte RM, He H, Arora J, Lu N, Tu XM *et al*. Posttraumatic stress disorder and suicide in 5.9 million individuals receiving care in the veterans health administration health system. *J Affect Disord* 2014; **166**: 1–5.
- 42 Lanius RA, Frewen PA, Girotti M, Neufeld RW, Stevens TK, Densmore M. Neural correlates of trauma script-imagery in posttraumatic stress disorder with and without comorbid major depression: a functional MRI investigation. *Psychiatry Res* 2007; **155**: 45–56.
- 43 Vialou V, Bagot RC, Cahill ME, Ferguson D, Robison AJ, Dietz DM *et al*. Prefrontal cortical circuit for depression- and anxiety-related behaviors mediated by cholecystokinin: role of Δ FosB. *J Neurosci* 2014; **34**: 3878–3887.
- 44 Daskalakis NP, Cohen H, Cai G, Buxbaum JD, Yehuda R. Expression profiling associates blood and brain glucocorticoid receptor signaling with trauma-related individual differences in both sexes. *Proc Natl Acad Sci USA* 2014; **111**: 13529–13534.
- 45 Vialou V, Robison AJ, LaPlant QC, Covington HE III, Dietz DM, Ohnishi YN *et al*. Δ FosB in brain reward circuits mediates resilience to stress and antidepressant responses. *Nat Neurosci* 2010; **13**: 745–752.



This work is licensed under a Creative Commons Attribution-NonCommercial-NoDerivs 4.0 International License. The images or other third party material in this article are included in the article's Creative Commons license, unless indicated otherwise in the credit line; if the material is not included under the Creative Commons license, users will need to obtain permission from the license holder to reproduce the material. To view a copy of this license, visit <http://creativecommons.org/licenses/by-nc-nd/4.0/>

Supplementary Information accompanies the paper on the Molecular Psychiatry website (<http://www.nature.com/mp>)